25. Lesher, C. M., Goodwin, A. M., Campbell, I. H. and Gorton, M. P., Trace element geochemistry of ore associated and barren felsic metavolcanic rocks in Superior Province, Canada. *Can. J. Earth Sci.*, 1985, **23**, 222–237.
26. Michard, A. and Albarede, F., The REE content of hydrothermal fluids. *Chem. Geol.*, 1986, **55**, 51–60.
27. Ugarkar, A. G., Archaean volcano-sedimentary hosted gold mineralisation in the Gadag gold field, western Dharwar craton, Southern India: An integrated view. *J. Appl. Geochem.*, 2002, **4**, 359–370.

ACKNOWLEDGEMENTS. The SEM–EDS analysis of monazite was done jointly by T.A.A.H., T.C.D. and T.A.A. at the Institute of Electron Optics, University of Oulu, Finland when T.C.D. was there on a Scholarship of the Finnish Centre for International Mobility awarded under Indo-Finnish exchange programme. We thank Mr Seppo Sivonen, Director, Institute of Electron Optics, for analytical facilities. A.G.U. was on Research Associateship and Pool Scientistship of CSIR, New Delhi when this study was carried out.

Received 8 February 2006; revised accepted 19 February 2007

Magnetovariational study over Lakshadweep Islands, southwestern continental margin of India

P. B. V. Subba Rao[1,*] and B. R. Arora[2]

[1]Indian Institute of Geomagnetism, Panvel, Navi Mumbai 410 218, India
[2]Wadia Institute of Himalayan Geology, Dehradun 248 001, India

The Chagos–Laccadive Ridge (CLR) is a prominent aseismic topographic feature in the northern Indian Ocean. The evolution and origin of the CLR continues to be a subject of great debate. Geomagnetic depth sounding studies have been carried out in five different Lakshadweep Islands. Transfer functions, summering relationship between anomalous and normal components of transient geomagnetic variations, by virtue of their sensitivity to sub-surface electrical conductivity distribution facilitate to constrain the deep structure and thermal state of the CLR.

The induction arrows over a wide range of periods indicates dominance of island effect. The residual induction arrows (obtained after accounting for the Island effect) suggest the concentration of anomalous induced currents in an elongated structure corresponding with track of the Reunion hotspot. Further, the thin sheet modelling of the residual induction arrows brings out a narrow belt of high-conductivity zone close to the eastern margin of the CLR. This is interpreted in terms of partial melt associated with the northward drifting of Indian plate over the Reunion mantle plume (65 Ma). The increase in the longitudinal conductance from north to south can be attributed to the degree of partial melting with younging of the age of volcanic intrusion to the south.

Keywords: Chagos–Laccadive Ridge, induction arrows, Lakshadweep Islands, Reunion hotspot.

THE southwestern continental margin of India comprises several tectonic features, including the Chagos–Laccadive Ridge (CLR), Pratap Ridge and a chain of grabens filled with sediments bordering the west coast of India. The CLR is a prominent aseismic topographic feature over which the Laccadive (Lakshadweep), Maldive and Chagos group of islands have formed. The Lakshadweep group of islands forms the northern part of the CLR and is parallel to the western continental margin of India.

Various theories have been proposed regarding the evolution of the CLR.

(a) Fisher *et al.*[1] and McKenzie and Sclater[2] associated the Chagos–Laccadive ridge with an old transform fault formed during the Cretaceous to Eocene period while India moved northward.
(b) Francis and Shor[3] have considered a hotspot origin for the ridge. This ridge was formed from the interaction of transiting Indian plate with the Reunion hotspot.
(c) Ben Avraham and Bunce[4] proposed diverse segmental origin for the CLR. The north and south segments have a volcanic origin, whereas the central part (Maldive segment) is a continental fragment drifted away from India.
(d) From the joint interpretation of seismic reflection and magnetic profiles, Naini and Talwani[5] and Harbison and Bassinger[6] suggested that the northern part of the CLR was a fragment of the Indian continent.
(e) Based on free-air anomaly and seismic profiles, Radha Krishna *et al.*[7] inferred that the northern part of the ridge formed a transition between continental crust and oceanic crust to the east and west respectively.

To constrain the nature of the crust beneath the northern part of the CLR, by conductivity imaging, we have carried out long-period magnetotelluric and geomagnetic depth sounding (GDS) experiments during April–May 2004 at five different Lakshadweep Islands (Figure 1). In this communication, we present the results obtained from the GDS experiment.

In GDS, deduction of the lateral conductivity distribution is based on the three components of the time-varying geomagnetic field, generally the geographic north (X), east (Y) and vertical (Z) components. The time-varying magnetic fields, which have their origin in the current systems in the ionosphere and distant magnetosphere, act as a natural source and induce secondary currents in the conductive layers of the earth. Transformation of the time-varying magnetic fields into frequency-dependent response functions is suitable for drawing qualitative and

*For correspondence. (e-mail: srao@iigs.iigm.res.in)

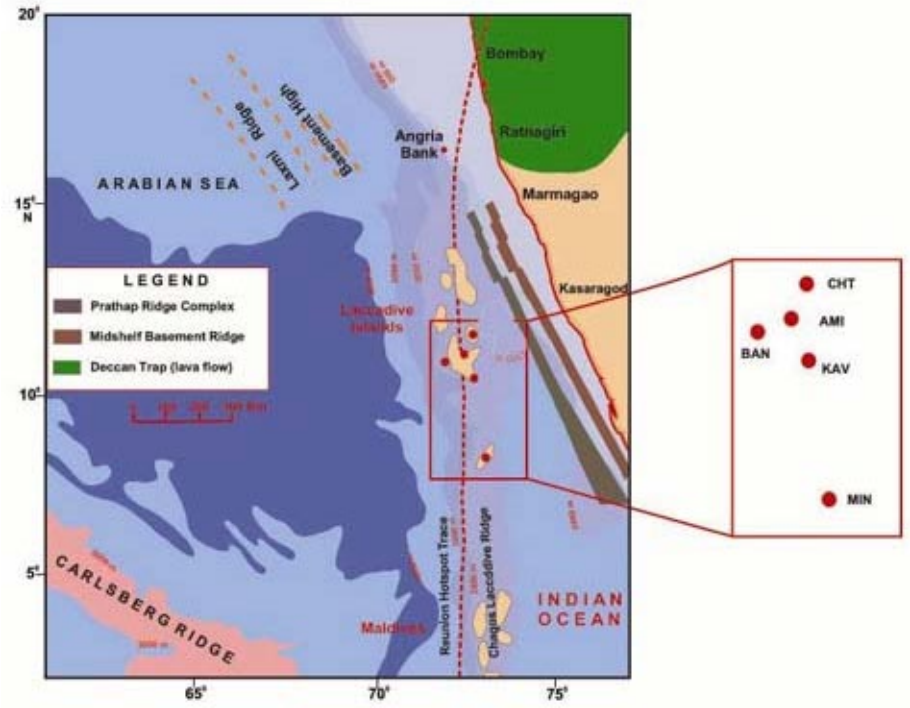

Figure 1. Map showing locations of GDS sites occupied in relation to the Chagos–Laccadive Ridge and trace of Reunion hotspot (dashed line) along the southwestern continental margin of India (after Subrahmanyam *et al*.[26]). The five different islands covered are Chetalat (CHT), Amini (AMI), Bangram (BAN), Kavaratti (KAV) and Minicoy (MIN).

quantitative deduction on conductivity distribution which is obtained through the transfer function formulation suggested by Schmucker[8]. At any given period, X_n, Y_n and Z_n represent the Fourier coefficients of the orthogonal magnetic fields. Then the observed magnetic field components at field site (X_o, Y_o and Z_o) can be represented into normal and anomalous parts ($X_o = X_n + X_a$). In such a case, frequency-dependent transfer functions that relate the anomalous field components at a given site with normal field components can be expressed as

$$Z_a = T_{zx}X_n + T_{zy}Y_n,$$

where T_{zx} and T_{zy} are the vertical field transfer functions. These transfer functions are obtained under the assumption of uniform source field for short-period fluctuations, where (a) Z_n is small compared with Z_a ($Z_n \to 0$); the entire observed Z could be treated as anomalous. (b) The anomalous parts of the horizontal fields are small, i.e. $X_a << X_n$ and $Y_a << Y_n$. (c) Z_n does not correlate with either X_n or Y_n. This allows cross-spectra terms between Z_a and X_n as well as with Y_n to be replaced by those between the total observed Z and X (or Y) fields.

Conventionally, the information contained in vertical transfer functions concerning the nature of conductivity distribution is extracted by presenting them as induction arrows. As T_{zx} and T_{zy} are complex functions, there exist two sets of induction arrows: corresponding to real (r) and quadrature (i) parts. The magnitude (S_r and S_i) and azimuth (ϕ_r and ϕ_i) of the arrow are given by:

$$S_r = \text{Sqrt}(\text{Real}(T_{zx})^2 + \text{Real}(T_{zy})^2),$$

$$S_i = \text{Sqrt}(\text{Imag}(T_{zx})^2 + \text{Imag}(T_{zy})^2),$$

$$\phi_r = \tan^{-1}(\text{Real}(T_{zy})/\text{Real}(T_{zx})),$$

$$\phi_i = \tan^{-1}(\text{Imag}(T_{zy})/\text{Imag}(T_{zx})).$$

It is usual to reverse the direction of real arrows so that they points towards the region of high internal electrical conductivity[9]. Hence when these arrows are displayed on the geographical grid of the stations, they form a powerful tool to locate and define the trend of the involved conductivity structures. For subsurface geoelectrical mapping of the CLR, three long-period magnetotelluric (LMT) and five fluxgate units were operated at different Lakshadweep Islands. The telluric fields could not be measured properly due to the high-contact resistance of electrodes with resistive coral reefs and due to the noise from the DC power supply. Therefore, estimation of magnetotelluric impedance tensors was difficult. Further, due to the encroachment of sea water during a cyclonic storm, data from two LMT and GDS sites were lost. In the present study, we present the results of the GDS data from four sites. Magnetic data from one LMT site (Chetalat, CHT) is also

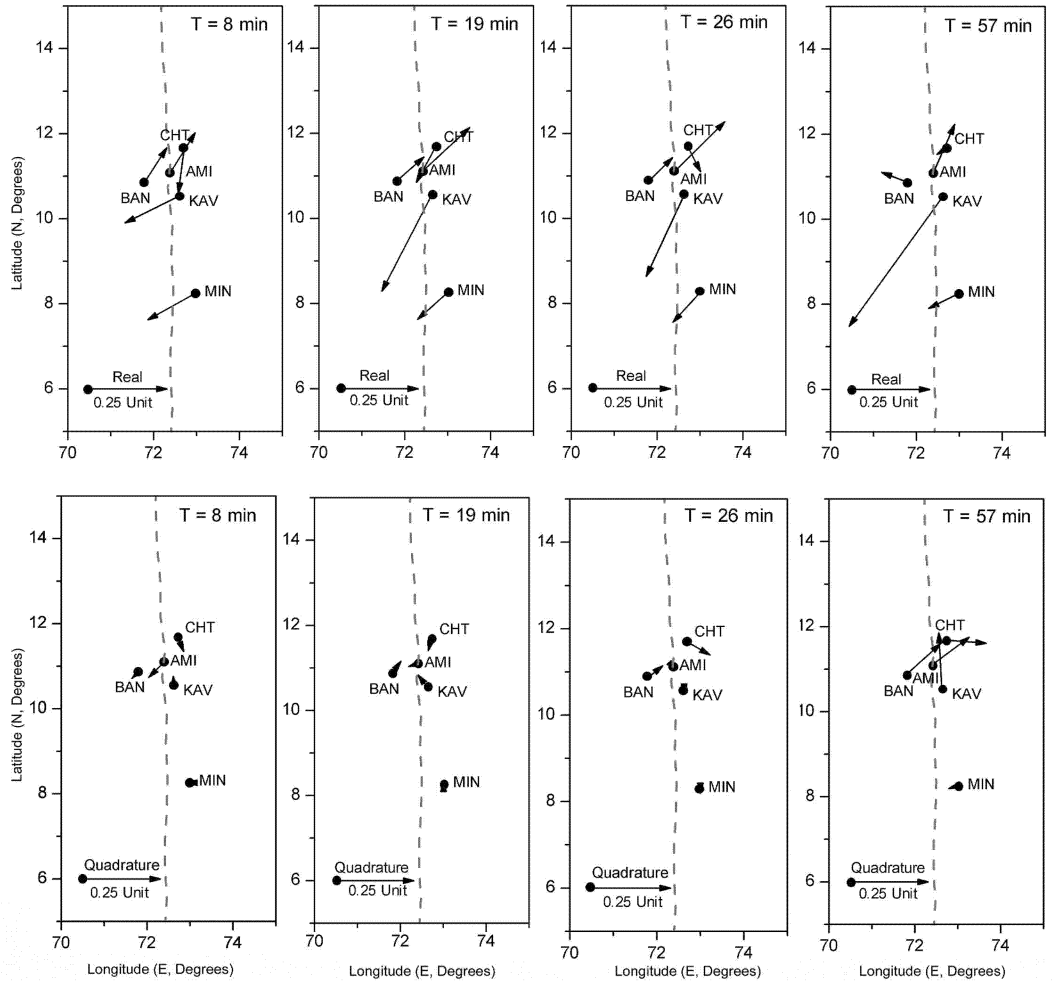

Figure 2. Observed induction arrows (real and quadrature) for four different periods at five different Lakshadweep Islands. Dashed line indicates trace of the Reunion hotspot.

employed. The observed induction arrows of Lakshadweep array are discussed next.

Night-time transient geomagnetic variations recorded at all five island sites (shown in Figure 1) have been considered. Robust regression analysis has been implemented in determing the single-station transfer functions. Vertical field single-station transfer functions are presented in the form of induction arrows and four sets of real and quadrature arrows for periods 8, 19, 26 and 57 min are shown in Figure 2. The observed induction arrows are relatively small at all sites. Each site is affected by the induction in the surrounding sea water due to the large land–sea electric conductivity contrast. This is known as Island effect and is caused by the perturbation of electric current induced in the sea surrounding the island.

The observed induction pattern is partly controlled by the trend of the bathymetry and local conductivity anomaly as evident from Bangram (BAN). At this site for short periods (19 min), the real induction arrows do not point towards deep sea. The induction arrows, with their NE–SW orientation, point at right angles to the local bathymetry as well as conductivity anomaly. Thus at short periods, the induction pattern is dominated by the conductivity anomaly of the islands. The magnitude of the NE oriented arrow diminishes progressively with increasing periods, vanishing almost around 43 min. At still longer periods (shown only for 57 min), they rotate anti-clockwise and point towards the deep sea (where the water column has a thickness over 3 km). At Kavaratti (KAV) and Minicoy (MIN), the induction arrows point towards deep sea in SE directions for all periods. At Chetalat (CHT) and Amini (AMI), the magnitudes of the observed induction arrows have been reduced due to 2 km deep sea water. This suggests that the observed induction pattern is dominated by the Island effect. Thus it is essential to estimate the same and eliminate from the observed induction response. The residual induction pattern thus estimated will be useful to infer the nature of deep crustal conductivity anomaly.

In the present study, for calculating the island effect, we have used the thin sheet algorithm developed by Vasseur and Weidelt[10]. This formulation requires that a region of normal structure must surround by the anomalous domain.

In the regional model, normal structure is represented by a conductive medium of 3300 S, equivalent to sea water of 1 km depth. The edge effect that arises due to artificially confining the observational (anomalous) domain by normal structure of uniform conductivity is minimized by extending the grid to sufficiently larger distances away from the observational domain[11]. Thin sheet of 5 km thickness with laterally varying conductance includes sea water as well as sediments of varying depths. This thin sheet is underlain by three-layers which have a resistivity of 200, 1000 and 10 Ωm, with a thickness of about 20 and 60 km respectively. The thicknesses of the various layers have been adopted based on gravity and seismic data analysis carried out by Radha Krishna *et al.*[7]. They considered the thick oceanic crust (15–20 km) underlain by a high-density underplated material and the thickness of the lithosphere ~80 km. For the purpose of conductance calculations[12], sea-water resistivity was taken to be 0.33 Ωm and that of the oceanic crust to be 200 Ωm. For deeper layers, the resistivity values have been taken from LMT investigations carried out in the western part of Dhawar craton[13]. They considered 150 km thick lithosphere of 1000 Ωm underlain by an asthenosphere having a resistivity of about 10 Ωm. Thus, we considered the resistivity values and thickness of different layers and carried out thin-sheet calculations.

For numerical calculations, the region between 71–80°E and 5–15°N (bathymetry is shown in Figure 1) was divided into a grid of 50×50 meshes, with a node spacing of about 25 km. For estimating the Island effect (arising due to land and sea water of variable depth), numerical computations have been carried out for a period range of 8–128 min. Figure 3 shows the real induction arrow pattern at 19 min, corresponding to the conductance distribution model depicting lateral variation associated with land and sea water of variable depth. The most dominant induction pattern is seen at the land–sea transition and persists for all periods. However, the presence of the Lakshadweep Islands in the Arabian Ocean produces strong perturbations in the flow path of induced currents in the oceanic region. As a result, the induction arrows point towards the deep ocean and are directed away from the land mass.

Residual induction arrows have been obtained by subtracting the modelled induction arrows (of oceanic response) from the observed induction arrows. The residual induction arrows obtained for four different periods are shown in Figure 4. These arrows show clear directional reversal between BAN and CHT with reduced magnitude at AMI. The reduced amplitude at AMI suggests concentration of induced currents in a conductive structure beneath AMI. The induction arrows at KAV and MIN point towards the Reunion hotspot trace and favour the presence of an elongated conductivity structure along the axis of the ridge.

Studying analytically the frequency response of 2D structures, Rokityansky[14], and Chen and Fung[15] noted that there exists a characteristic period T_c at which quadrature arrows flip their sign and at this period, the modulus of the real induction arrows is maximum. T_c is used to estimate the longitudinal conductance ($G = \sigma Q\, S$).

$$G = 5 \times 10^4 \times (T_c)^{1.2},$$

where σ is the conductivity (S/m) and Q is cross-sectional area ($Q = h \times l$ in sq. m) of the anomalous conductivity body. The above relationship is site-dependent. However, as the site for which the above relation was derived is not much different from that of the present study area, we adopted the above relation as it is.

In the present study, the real induction arrows acquire a peak value in the period range of 19–26 min. In this period range, the quadrature arrows have nearly vanishing amplitudes and their direction get reversed above and below this period (as seen at BAN and MIN stations). This critical period (T_c = 19 min) at which real arrows tend to be maximum and quadrature arrows flip their direction is characteristic of the anomalous body. Using the relation given above, the estimated longitudinal conductance of the anomalous conductivity structure is about 2.32×10^8 S.

Frequency characteristics of real and quadrature induction arrows for BAN and MIN (located on either side of the Lakshadweep Ridge) are shown in Figure 5. Maximum amplitude of the real induction arrow is seen at 19 min for BAN and 26 min for MIN. The amplitude of quadrature induction arrows becomes minimum at this

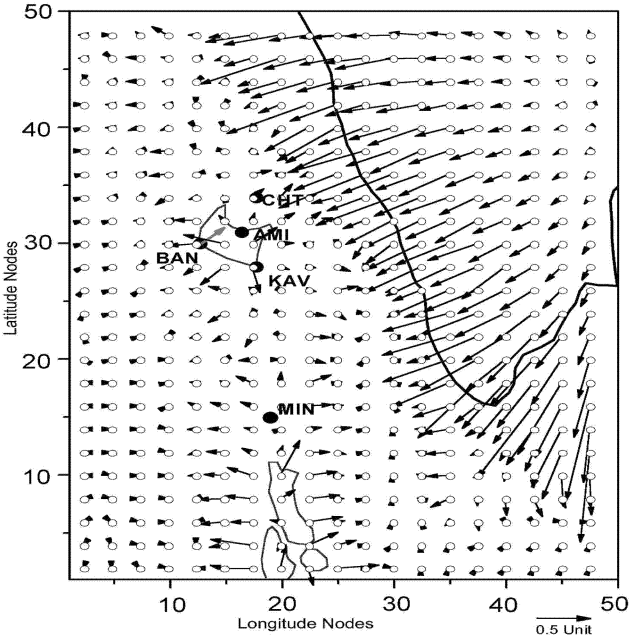

Figure 3. Calculated real induction arrows at a period of 19 min. They portray lateral variation in conductances due to land and sea water of variable depth. The arrows are shown for alternate grid points. Grey arrow at BAN shows the observed real induction arrow at 19 min and its scale has been doubled.

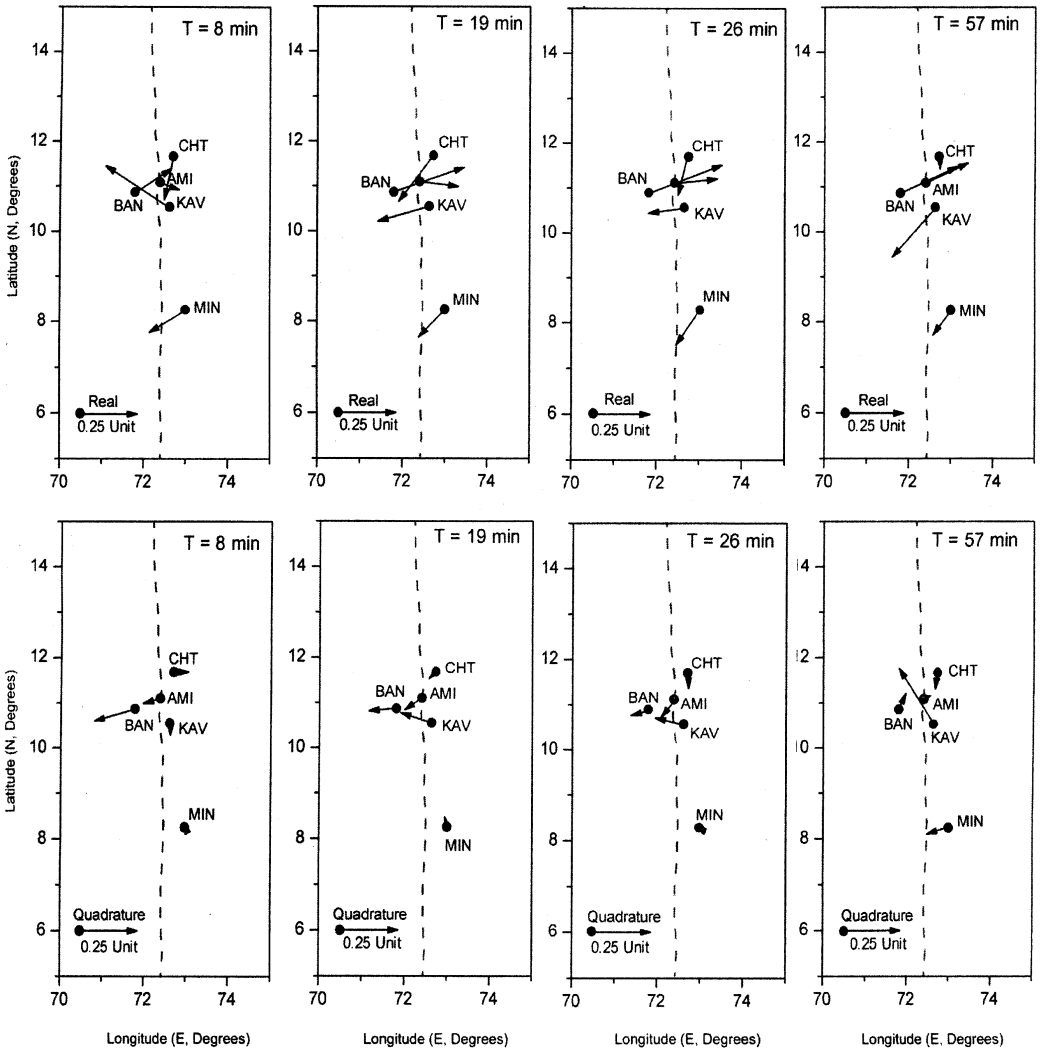

Figure 4. Residual induction arrows for four different periods.

characteristic period. This suggests that the anomalous conductivity structure becomes more conductive from north to south of the Lakshadweep Ridge.

Induction arrows at relatively long periods are sensitive to local and regional conductivity structures. Recently, integration of large-scale magnetometer array data over the entire southern peninsular India, as well as ocean bottom magnetometer array data in the Bay of Bengal has helped to develop a regional electrical conductivity distribution model[16,17]. This regional anomaly, named South India Offshore Conductivity Anomaly (SIOCA), correlates with low-velocity zone, low magnetization anomaly and a strong negative geoid, all centred near the southern tip of India. This regional anomaly has been attributed to the manifestations of the interaction of Marion plume outburst with Indian lithosphere. The position of the anomaly corresponds well with the location of the Marion plume outburst that led to the separation of India and Madagascar[18]. Its extension towards NE and NW are the anomalous conductive structures in the Palk Strait (PC) and underneath Comorin Ridge (CRC).

Both Island effect and Coast effect are due to the sharp conductivity contrast between land and sea. This results in the perturbation of induced currents in conducting sea water. If the Island/Coast effect is removed, one can expect to see the characteristics of any local subsurface anomalous conductor in the residual induction arrows. In order to know the nature of the local anomalous conductor, it is critical to include influence of regional map structure as detailed above (SIOCA).

In order to explain the residual induction arrows by thin-sheet model of laterally varying conductance, the region between 70°–80°E and 5°–15°N was divided into 50×50 meshes, with a grid spacing of 25 km. Since the effect of sea water has been accounted for in the calculations of Island effect, the thin-sheet numerical calculations were carried out by replacing sea water with the land material having a resistivity of about 200 Ωm.

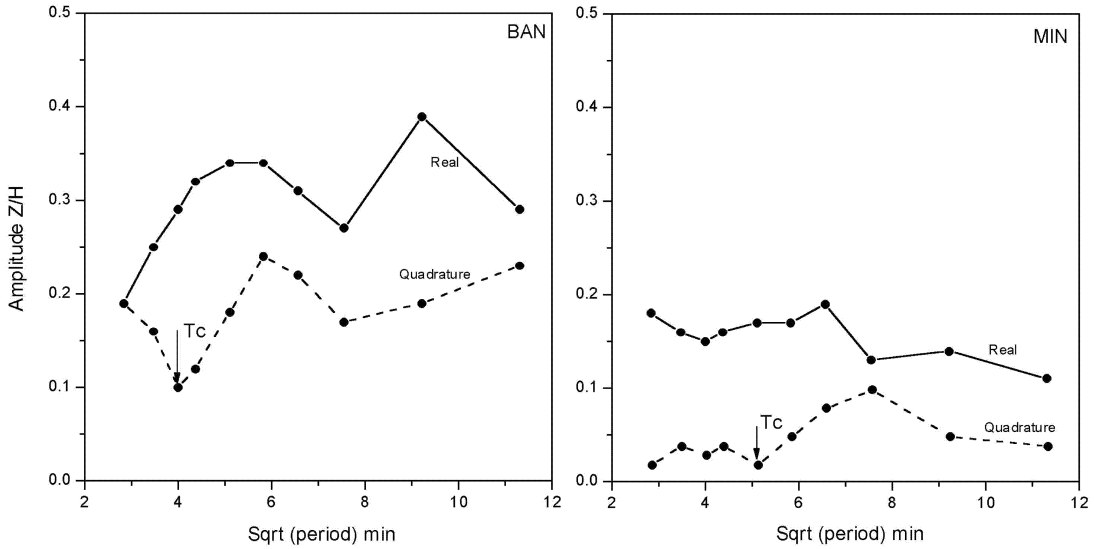

Figure 5. Changes in magnitude of real (solid) and quadrature (dashed) arrows as a function of square root of period shown for stations BAN (left) and MIN (right). These sites lie on either side of the Lakshadweep ridge. An arrow points the characteristic period T_c.

The residual induction arrows have been explained in terms of high-conductivity anomaly running parallel to the trace of hotspot, which has a conductance of about 10,000 S in the north that increases to 20,000 S towards south. The thickness as well as depth of the conductivity body increases towards MIN. The reversal in induction arrows between CHT and BAN has been explained in terms of high-conductivity anomaly, having a conductance of about 10,000 S with a reduction at AMI. The induction arrow at KAV is due to the high conductivity anomaly following the track of Reunion hotspot that extends towards MIN.

Movement of the Indian lithosphere plate over a Reunion mantle plume[19], produced a chain of volcanic islands (Laccadive and Maldive Islands) during 45–60 Ma. Thermal remobilization/reactivation during this period may have increased the mantle temperature beneath the CLR[20], which is higher than normal by 100–250°C. Using shear wave velocity, Manglik[21] studied the anomalous character of the lithosphere beneath the CLR. He suggested a low-velocity zone that decreases from south to north (25–15 km). Asalatha *et al.*[22] observed thick crustal roots beneath the CLR on the basis of admittance analysis. The presence of such thick high-density material is consistent with the gravity modelling carried out by Radhakrishna *et al.*[7]. They interpreted this gravity high in terms of high-density mantle material underplating beneath the CLR.

The zone of low seismic velocity, high mantle temperature and underplating mantle material beneath the CLR is not necessarily coincident with depth, may symbolize partial melt of crustal and mantle material associated with the hotspot volcanism. Further, as a consequence of the above, during long geological time, this process might have released hydrous fluids/volatiles forming an additional source for the enhanced conductivity. Given strong dependence of electrical conductivity on temperature, as seen from the conductance map (Figure 6), it can be inferred that thermal activity decreases from south to north of the Lakshadweep group of islands and coincides with the low-velocity zone as mapped by Manglik[21].

Thin-sheet model required a conductance of the order of 10,000–20,000 S to simulate the Reunion hotspot trace. Thus, the observed conductivity anomaly along the hotspot trace can be attributed to the section of the crust/mantle that has been thermally remobilized or altered by Reunion hotspot activity. The conductivity anomaly at AMI can be attributed to the narrow magma conduits related to magma transport though the uppermost mantle and lower crust.

Elsewhere, EM studies have been carried out around Society Islands[23] and across the Hawaiian hotspot swell[24,25]. In the above studies, the mapped high conductivity has been explained by partial melt. For the Hawaiian plume[24], the estimated conductance is of the order of 25,000–40,000 S, having a temperature of about 1460°C. In our study, the estimated lower conductance (10,000–20,000 S) for the Reunion hotspot track seems to be consistent with the fact that plume–lithosphere interactions were initiated ~40–50 Ma.

In conclusion, magnetovariational studies over the Lakshadweep Islands support the hypothesis of hotspot origin for the northern part of the CLR. Given the poor depth resolution of GDS, the conductance model developed provides depth-integrated conductance. The depth extent of conductivity anomaly associated with the Lakshadweep Islands still remains elusive. Seafloor EM measurements (across the CLR) supplemented by magnetotelluric sound-

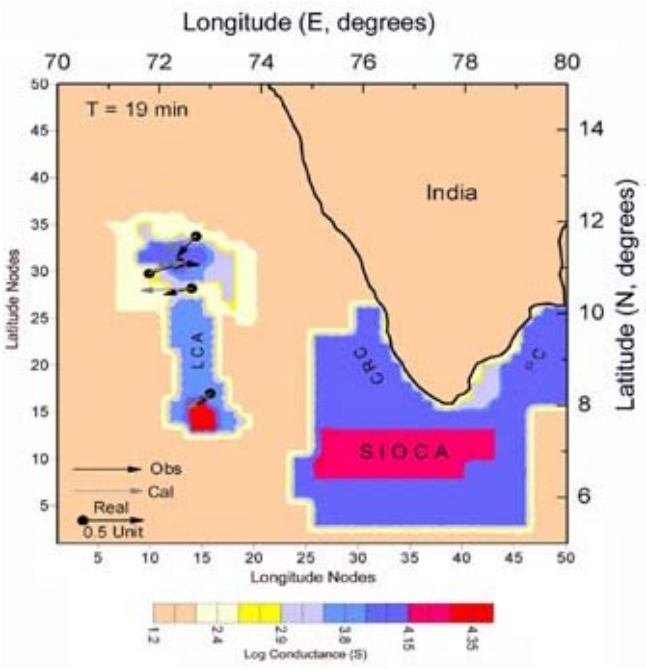

SIOCA	South Indian Offshore Conductivity Anomaly
PC	Palk Strait Conductor
CRC	Comorin Ridge Conductor
LCA	Lakshadweep Conductivity Anomaly

Figure 6. Thin-sheet conductance (logarithmic scale) map for Lakshadweep Islands (northern part of the Chagos–Laccadive Ridge) and adjoining oceanic region. Regional anomaly SIOCA as discussed in the text is also included for numerical calculations. Comparison of observed and calculated real induction arrows is shown for 19 min.

ings over the Lakshadweep group of islands will be useful in determining the electrical conductivity distribution on either side of the CLR and its evolutionary processes.

1. Fisher, R. L., Sclater, J. G. and Mckenzie, D. P., Evolution of the central Indian ridge, western Indian Ocean. *Bull. Geol. Soc. Am.*, 1971, **82**, 553–562.
2. Mckenzie, D. and Sclater, J. G., The evolution of the Indian Ocean since the late Cretaceous. *Geophys. J. R. Astron. Soc.*, 1971, **25**, 437–528.
3. Francis, T. J. G. and Shor, G. C., Seismic refraction measurements in the northwest Indian Ocean. *J. Geophys. Res.*, 1974, **71**, 7427–7449.
4. Ben Avraham, Z. and Bunce, E. T., Geophysical studies of the Chagos–Laccadive Ridge, Indian Ocean. *J. Geophys. Res*., 1977, **82**, 1295–1305.
5. Naini, B. R. and Talwani, M., Structural framework and evolutionary history of the continental margin of western India. In *Studies in Continental Margin Geology* (eds Wakins, J. S. and Drake, C. L.), Am. Assoc. Pet. Geol. Mem, 1982, vol. 34, pp. 167–191.
6. Harbison, R. N. and Bassinger, B. G., Marine geophysical studies off western India. *J. Geophys. Res.*, 1973, **78**, 432–440.
7. Radha Krishna, M., Verma, R. K. and Purushotham, A. K., Lithospheric structure below the eastern Arabian Sea and adjoining west coast of India based on integrated analysis of gravity and seismic data. *Mar. Geophys. Res*., 2002, **23**, 25–42.
8. Schmucker, U., Anomalies of geomagnetic variations in the southwestern United States. *Bull. Scripts Inst. Oceanogr.*, 1970, **13**, 1–165.
9. Lilley, F. E. M. and Arora, B. R., The sign convention for quadrature Parkinson arrows in geomagnetic induction studies. *Rev. Geophys. Space Phys.*, 1982, **20**, 513–518.
10. Vasseur, G. and Weidelt, P., Bimodal electromagnetic induction in non-uniform thin sheets with an application to the northern Pyrenean induction anomaly. *Geophys. J. R. Astron. Soc.*, 1977, **51**, 669–690.
11. Mareschal, M., Vasseur, G., Srivastava, B. J. and Singh, R. N., Induction models of southern India and effect of offshore geology. *Phys. Earth Planet. Inter*., 1987, **45**, 137–148.
12. Heinson, G. S. and Lilley, F. E. M., An application of thin sheet electromagnetic modeling to the Tamsan Sea. *Phys. Earth Planet. Inter*., 1993, **81**, 231–251.
13. Arora, B. R., Rawat, G., Subba Rao, P. B. V., Maurya, R. N. and Iyengar, R. V., Long period magnetotelluric measurements in the Dharwar craton, South India. Joint IAGA & IASPEI Assembly, Hanoi, 19–31 August 2001.
14. Rokityansky, I. I., *Geomagnetic Investigations of the Earth's Crust and Mantle*, Springer Verlag, Berlin, 1982.
15. Chen, P. F. and Fung, P. C. W., On the behavior of the imaginary Parkinson arrows near the anomalous conductive–host medium interface. *Phys. Earth Planet. Inter*., 1987, **50**, 195–198.
16. Arora, B. R. and Subba Rao, P. B. V., Integrated modeling of EM response functions from peninsular India and Bay of Bengal. *Earth Planets Space*, 2002, **54**, 637–654.
17. Arora, B. R., Subba Rao, P. B. V. and Nagar, V., Electrical conductivity signatures of plume–lithosphere interactions in the Indian Ocean. *Mem. Geol. Soc. India*, 2003, **53**, 393–418.
18. Storey, B. C., The role of mantle plumes in continental breakup: Case histories from Gondwanaland. *Nature*, 1995, **377**, 301–308.
19. Vandamme, D. and Courtillot, V., Palaeomagnetism of Leg 115 basement rocks and latitudinal evolution of the Réunion hotspot. *Proc. ODP Sci. Res*., 1990, **115**, 111–117.
20. Henstock, T. J. and Thompson, P. T., Self-consistent modeling of crustal thickness at Chagos–Laccadive ridge from bathymetry and gravity data. *Earth Planet. Sci. Lett.*, 2004, **224**, 325–336.
21. Manglik, A., Shear wave velocity structure of the upper mantle under the NW Indian Ocean. *J. Geodyn.*, 2002, **34**, 615–625.
22. Asalatha, B., Subrahmanyam, C. and Singh, R. N., Origin and emplacement of Chagos–Laccadive Ridge, Indian Ocean, from admittance analysis of gravity and bathymetry data. *Earth Planet. Sci. Lett*., 1991, **105**, 47–54.
23. Nolasco, R., Tarits, P., Filloux, J. H. and Chave, A. D., Magnetotelluric imaging of the Society Islands hotspot. *J. Geophys. Res*., 1998, **103**, 30287–30309.
24. Simpson, F., Steveling, E. and Leven, M., The effect of the Hawaiian plume on the magnetic daily variation. *Geophys. Res. Lett*., 2000, **27**, 1775–1778.
25. Constable, S. and Heinson, G., Hawaiian hot-spot swell structure from seafloor MT sounding. *Tectonophysics*, 2004, **389**, 111–124.
26. Subrahmanyam, V., Gopal Rao, D., Ramana, M. V., Krishna, K. S., Murthy, G. P. S. and Gangadhara Rao, M., Structure and tectonics of the southwestern continental margin of India. *Tectonophysics*, 1995, **249**, 267–282.

ACKNOWLEDGEMENTS. We thank the Department of Science and Technology, New Delhi for supporting the project. Assistance from Mr D. M. Daga during fieldwork is acknowledged. We thank Dr A. K. Singh for providing us the fluxgate magnetometer data of LMT site. We are grateful to Dr M. S. Syed Ismail Koya, Deputy Director (and his team members), DST; Administration of the Union Territory of the Lakshadweep, Kavaratti, for providing necessary help to carrying out the experiments successfully. We thank the referee for his valuable comments that helped improve this manuscript.

Received 25 April 2005; revised accepted 15 February 2007